Scattering mechanisms in state-of-the-art GaAs/AlGaAs quantum wells

Yi Huang (黄奕) ●,* B. I. Shklovskii, and M. A. Zudov

School of Physics and Astronomy, University of Minnesota, Minneapolis, Minnesota 55455, USA

Motivated by recent breakthroughs in molecular beam epitaxy of GaAs/AlGaAs quantum wells [Y. J. Chung *et al.*, Nat. Mater. **20**, 632 (2021)], we examine contributions to mobility and quantum mobility from various scattering mechanisms and their dependencies on the electron density. We find that at lower electron densities, $n_e \lesssim 1 \times 10^{11}$ cm^{-2}, both transport and quantum mobility are limited by unintentional background impurities and follow a power-law dependence, $\propto n_e^\alpha$, with $\alpha \approx 0.85$. Our predictions for quantum mobility are in reasonable agreement with an estimate obtained from the resistivity at filling factor $\nu = 1/2$ in a sample of Y. J. Chung *et al.* with $n_e = 1 \times 10^{11}$ cm^{-2}. Consideration of other scattering mechanisms indicates that interface roughness (remote donors) is likely a limiting factor of transport (quantum) mobility at higher electron densities. Future measurements of quantum mobility should yield information on the distribution of background impurities in GaAs and AlGaAs.

Advances in molecular beam epitaxy, particularly the purification of source materials and improved vacuum conditions, have recently lead to another generation of GaAs/AlGaAs quantum wells [1] in which the mobility reached a record value of $\mu = 4.4 \times 10^7$ cm^2 V^{-1} s^{-1} at electron density $n_e = 2.0 \times 10^{11}$ cm^{-2}. The increase in mobility was especially pronounced at lower densities ($n_e \lesssim 1 \times 10^{11}$ cm^{-2}), where μ was twice the previously reported record values. At higher densities ($n_e \gtrsim 2 \times 10^{11}$ cm^{-2}), however, the mobility has decreased to $\mu \approx 3.5 \times 10^7$ cm^2 V^{-1} s^{-1} at $n_e \approx 2.7 \times 10^{11}$ cm^{-2}, approaching previously reported values. While the increase of μ at low n_e could be readily attributed to a reduced concentration of unintentional background impurities, subsequent reduction of μ at higher n_e calls for revisiting other scattering sources.

In this Letter, we theoretically examine both transport and quantum mobility (μ_q) considering scattering by background impurities (BIs), remote ionized donors in the doping layers (RI), interface roughness (IR), and alloy disorder (AD). We find that both μ and μ_q are limited by BI scattering at low n_e, as expected. With increasing n_e, however, scattering on IR (and eventually on AD) becomes important, as far as μ is concerned, whereas μ_q becomes limited by RI scattering [2].

Modern GaAs-based heterostructures, such as those reported in Ref. [1], consist of a GaAs quantum well of width w surrounded by Al$_x$Ga$_{1-x}$As barriers of thickness d. A two-dimensional electron gas (2DEG) with a concentration n_e is supplied by two remote doping layers, each located at a distance $d_w = d + w/2$ from the center of the GaAs quantum well. These layers have a sophisticated doping well design, which helps to substantially reduce the scattering by ionized donors owing to excess electron screening [3–6]. In this design, a $\delta-$ layer of silicon atoms with concentration

$n \gg n_e$ is implanted into a narrow ($\approx$3 nm) GaAs quantum well, which is sandwiched between thin ($\approx$2 nm) AlAs layers [7]. In our calculations, we use $n \approx 1.5 \times 10^{12}$ cm^{-2}, Al mole fraction $x = 0.12$, and take into account the electron density dependencies of the effective spacer thickness d_w and of the quantum well width w. More specifically, we use $k_F w = 3.9$, where $k_F = \sqrt{2\pi n_e}$ is the Fermi wave number and $d_w^{-1} = a n_e$, where $a = 3.55$ nm [8]. These constraints were obtained by fitting samples parameters of Ref. [1], as detailed in the Supplemental Material [9].

We start with transport mobility, $\mu = e\tau/m^\star$, where $m^\star = 0.067\,m_0$ is the effective mass of an electron in GaAs [10], m_0 is the free electron mass,

$$\frac{1}{\tau} = \frac{4m^\star}{\pi \hbar^3} \int_0^{2k_F} \frac{dq}{\sqrt{4k_F^2 - q^2}} \left(\frac{q}{2k_F}\right)^2 \langle |U(q)|^2 \rangle, \quad (1)$$

is the transport scattering rate, and $U(q)$ is the screened potential of a given scattering source.

Coulomb background impurities. The screened potential squared averaged over impurity positions is given by

$$\langle |U_{\text{BI}}(q)|^2 \rangle = \int_{-\infty}^{+\infty} dz\, N(z) U_1^2(q, z), \quad (2)$$

where $U_1^2(q, z)$ is the screened potential squared from a single Coulomb impurity, and $N(z)$ is the 3D concentration of impurities at a distance z from the center of the 2DEG. Since the main contribution to momentum relaxation comes from impurities located close to the quantum well, for which excess electron screening [3] is not important and $U_1(q, z)$ can be obtained taking into account screening by electrons in the quantum well only. Using Thomas-Fermi (TF) approximation [3], and following Refs. [11–15], we can write (more detailed discussion can be found in the Supplemental
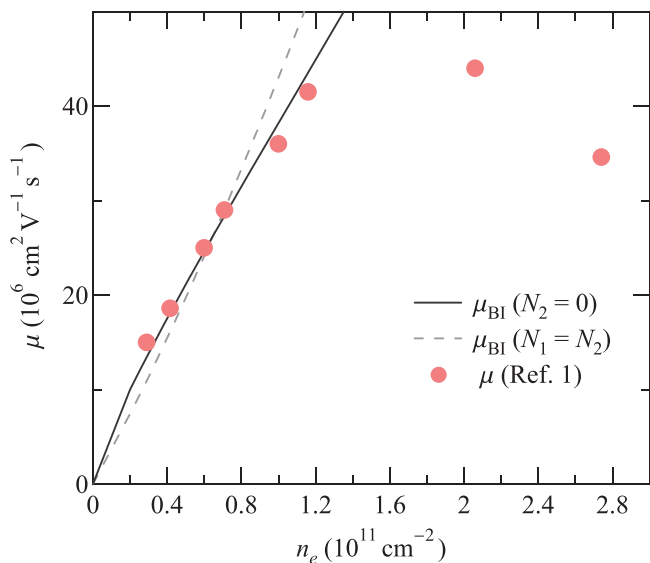
*Corresponding author: huan1756@umn.edu

FIG. 1. Mobility μ versus electron density n_e. Circles are experimental data from Ref. [1]. Solid (dashed) line represents μ_{BI} calculated for $N_1 = 1.4 \times 10^{14}$ cm^{-3}, $N_2 = 0$ ($N_1 = N_2 = 5 \times 10^{12}$ cm^{-3}).

Material [9])

$$U_1(q, z) = \frac{2\pi e^2}{\kappa q \epsilon(q)} \int_{-\infty}^{+\infty} dz' \, |\psi(z')|^2 e^{-q|z-z'|}, \qquad (3)$$

where $\psi(z)$ is the wave function along z direction and the dielectric function is given by

$$\epsilon(q) = 1 + (q_{\text{TF}}/q) F_c(qw)[1 - G(q)]. \qquad (4)$$

Here, $q_{\text{TF}} = 2/a_B$, $a_B = \kappa \hbar^2/m^\star e^2$ is the effective Bohr radius, $\kappa = 12.9$ is the dielectric constant of GaAs, $G(q) = q/(2\sqrt{q^2 + k_F^2})$ is the local field correction using Hubbard approximation [11], and the form factor $F_c(qw)$ is given by

$$F_c(qw) = \iint_{-\infty}^{+\infty} dz dz' |\psi(z)|^2 |\psi(z')|^2 \exp(-q|z - z'|). \quad (5)$$

For small concentration $n_e < 1 \times 10^{11}$ cm^{-2}, it suffices to use an infinite-potential-well approximation and $\psi(z) = \sqrt{2/w} \cos(z\pi/w) \Theta(w/2 - |z|)$ in both Eqs. (3) and (5).

Following Ref. [3], we define BI density as

$$N(z) = \begin{cases} N_1, & w/2 < |z| < d_w \\ N_2, & |z| < w/2, \end{cases} \qquad (6)$$

where N_1 (N_2) represents the 3D concentration of impurities in AlGaAs (GaAs). The results of our calculations for uniform impurity distribution ($N_1 = N_2$) and for no impurities in GaAs ($N_2 = 0$) are shown in Fig. 1 along with the experimental data of Ref. [1] (circles). We find that the data at $n_e \lesssim 1 \times 10^{11}$ cm^{-2} can be better described by $N_1 = 1.4 \times 10^{14}$ cm^{-3} and $N_2 = 0$ (solid line). Assuming uniform distribution of impurities (dashed curve) yields $N_1 = N_2 = 5 \times 10^{12}$ cm^{-3}, which is close to an estimate 1×10^{13} cm^{-3} of Ref. [1] ([16]). We also note that $\mu_{\text{BI}}(N_2 = 0)$ is well described by $\mu_{\text{BI}} = 38.3 \, n_e^\alpha$, where $\alpha \approx 0.85$, whereas $\mu_{\text{BI}}(N_1 = N_2)$ follows $\mu_{\text{BI}} = 43.1 \, n_e^\alpha$, where $\alpha \approx 1.12$. Here and in what

follows we assume that the electron density is in units of 10^{11} cm^{-2} and the mobility is in units of 10^6 cm^2 V^{-1} s^{-1}.

While BI scattering can describe the experimental data reasonably well at $n_e \leqslant 1$, it is clear that BI scattering alone cannot explain experimental μ at higher n_e. Indeed, obtained power laws represent crossovers from $\mu_{\text{BI}} \propto n_e^{1/2}$ at low n_e [3] to $\mu_{\text{BI}} \propto n_e^{3/2}$ at higher n_e [18]. To explain the experimental μ at higher n_e, one needs to examine other scattering sources.

Remote impurities. One obvious candidate for reduced μ at higher n_e is RI impurity scattering. For electron densities $n_e < 10$ and for a given doping concentration $n = 1.5 \times 10^{12}$ cm^{-2}, the fraction of ionized donors in each doping layer is small, $1 - f = n_e/2n < 0.5$, and we can use Eq. (22) from Ref. [3] ([19]),

$$\mu_{\text{RI}} = 7.7 \frac{e}{\hbar} \frac{n k_F^3 d_w^5}{n_e} = 1.6 \times 10^6 \, n_e^{-9/2}, \qquad (7)$$

where in the final expression of Eq. (7) we used $n = 15$, $k_F = \sqrt{2\pi n_e}$, and $d_w^{-1} = a n_e$ [8]. Equation (7) gives $\mu_{\text{RI}} \sim 10^4$ at $n_e = 3$, which is more than 300 times larger than experimental μ, so the RI scattering is still irrelevant in this regime. We note, however, that additional mechanisms of disorder in the doping layers may lead to an increase of RI scattering, as discussed in Sec. V of Ref. [3], although quantitative understanding of these mechanisms is still lacking.

Interface roughness. Scattering on IR originates from fluctuations of the ground-state energy due to $1 - 2$ monolayer local variations of the quantum well width w. For the infinite barrier height ($V \rightarrow \infty$), the corresponding transport scattering rate $\tau_{\text{IR}}^{-1} \propto w^{-6}$ [12,13] and such dependence was confirmed in narrow $w < 10$ nm GaAs quantum wells with AlAs barriers [20,21]. However, in Al$_x$Ga$_{1-x}$As/GaAs quantum wells, the barrier height is significantly reduced ($V \approx 0.75x$ eV for $x < 0.45$), and fluctuations of the ground-state energy are diminished due to finite penetration of the electron wave function into the barrier [14,22]. As a result, τ_{IR}^{-1} is considerably suppressed compared to the case $V \rightarrow \infty$, and its dependence on w weakens [21–24].

We calculate the IR-limited scattering rates following the approach of Refs. [14,22]. We use the barrier height for $x = 0.12$ and take into account the difference in the electron effective mass in the GaAs well ($m^\star = 0.067 \, m_0$) and in the Al$_{0.12}$Ga$_{0.88}$As barriers ($m_B = (0.067 + 0.083x)m_0 = 0.077 m_0$). At the end, we also impose a constraint $k_F w = 3.9$ [8].

Using the correlator of local well-width variations $\langle \Delta(\mathbf{r})\Delta(\mathbf{r}') \rangle = \Delta^2 \exp(-|\mathbf{r} - \mathbf{r}'|^2/\Lambda^2)$, where Δ is the roughness height and Λ is the roughness lateral size, the scattering potential due to interface roughness is given by

$$\langle |U_{\text{IR}}(q)|^2 \rangle = \frac{\pi}{\epsilon^2(q)} \Delta^2 \Lambda^2 \left(\frac{\partial E}{\partial w} \right)^2 e^{-q^2\Lambda^2/4}, \qquad (8)$$

where E is the ground-state energy for the finite potential well. Here, the dielectric function $\epsilon(q)$, see Eq. (4), is computed with the form factor $F_c(qw)$, see Eq. (5), using finite-potential-well wave function. (See Supplemental Material for details [9].)

By substituting Eq. (8) into Eq. (1), we obtain the mobility due to interface roughness μ_{IR} as shown in Fig. 2. To
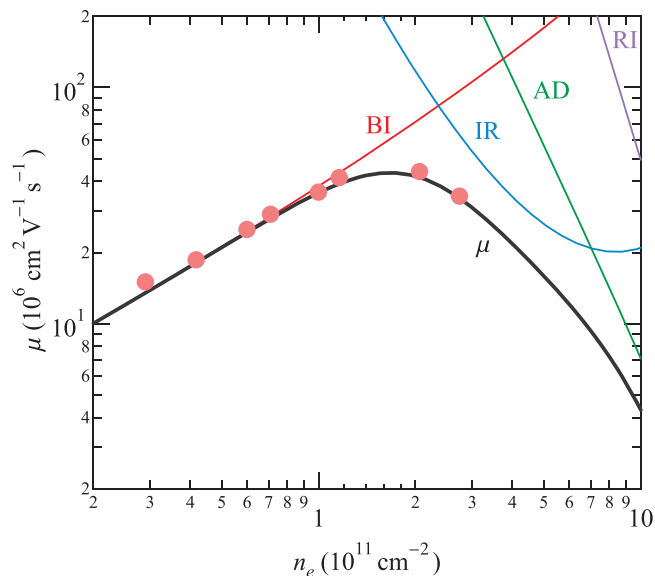
FIG. 2. Mobility μ versus electron density n_e. Circles are experimental data from Ref. [1]. Thin lines marked by BI, IR, AD, and RI represent μ_{BI} ($N_1 = 1.4 \times 10^{14}$ cm^{-3}, $N_2 = 0$), μ_{IR} ($\Delta = 0.283$ nm, $\Lambda = 8$ nm, $x = 0.12$), μ_{AD} ($x = 0.12$), and μ_{RI} [Eq. (7)], respectively. Thick line represents μ limited by all contributions.

reproduce the experimental data at $n_e > 2$, we arrived at $\Delta = 2.83$ Å and $\Lambda = 80$ Å. With these roughness parameters, μ_{IR} becomes equal to $\mu_{BI}(N_2 = 0)$ at $n_e \approx 2.4$ and, in the vicinity of this density, can be described by $\mu_{IR} \simeq 4.7 \times 10^2 \, n_e^{-2}$. We have also examined the effect of x on the mobility limited by IR. By raising x from 0.12 to 0.24, a value which is common for previous generation of samples, μ_{IR} at $n_e = 3$ becomes smaller by 24%, although this effect weakens at lower n_e.

Alloy disorder. AD scatters electrons due to the wave function tails extending into the Al$_x$Ga$_{1-x}$As barriers. Usually, in typical high mobility samples, this scattering mechanism is deemed irrelevant, see e.g., Refs. [22,25]. However, in light of lower x used in the new generation of samples [1], it is important to revisit this scattering source. Following Refs. [15,22,26], we write the scattering potential as

$$\langle |U_{AD}(q)|^2 \rangle = \frac{(\Delta E_c)^2}{\epsilon^2(q)} \Omega x(1-x) \int_{|z|>w/2} |\psi(z)|^4 dz, \quad (9)$$

where $\Omega = a^3/4$, $a = 5.67$ Å is the lattice constant and $\Delta E_c \simeq 1$ eV is the conduction band discontinuity at the Γ-point of GaAs/AlAs interface. As for the case of IR, we use a finite-potential-well wave function to calculate the form factor in $\epsilon(q)$ (see Supplemental Material [9]). Substituting Eq. (9) into Eq. (1) and applying the constraint $k_F w = 3.9$ [8], we obtain the mobility limited by AD scattering μ_{AD} as shown in Fig. 2. We note that μ_{AD} can be well described by $\mu_{AD} \simeq 7.1 \times 10^3 \, n_e^{-3}$ and that it becomes equal to μ_{BI} at $n_e \approx 3.7$ and to μ_{IR} at $n_e \approx 7$. We thus conclude that AD scattering cannot be ignored at higher densities. We have also examined the effect of x on mobility limited by AD. By increasing x from 0.12 to 0.24, μ_{AD} increases by a factor of 2.4 for $n_e < 10$.

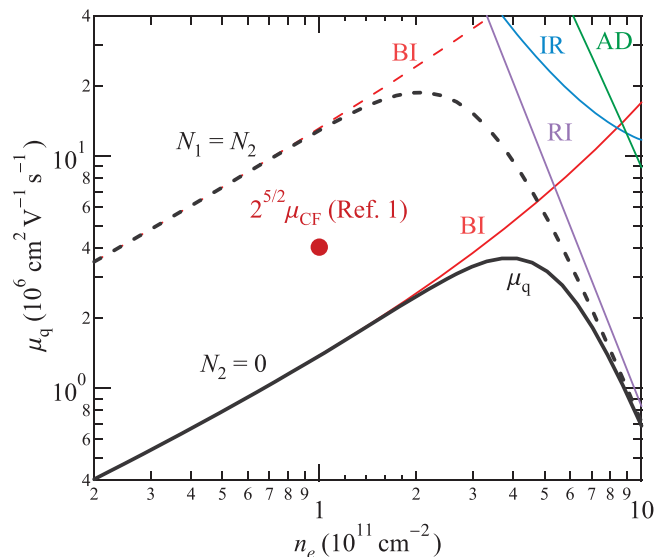We now turn to the effects of different scattering mechanisms on quantum mobility $\mu_q = e\tau_q/m^\star$, where the quantum

FIG. 3. Quantum mobility μ_q versus electron density n_e. Thin solid lines marked by BI, IR, AD, and RI represent $\mu_{q,BI}$ ($N_1 = 1.4 \times 10^{14}$ cm^{-3}, $N_2 = 0$), $\mu_{q,IR}$ [$\Delta = 0.283$ nm, $\Lambda = 8$ nm, $x = 0.12$), $\mu_{q,AD}$ ($x = 0.12$), and $\mu_{q,RI}$ (Eq. (11)], respectively. Thick solid line represents μ_q limited by all contributions. Thick dashed line is μ_q limited by all contributions but with $\mu_{q,BI}$ computed for $N_1 = N_2 = 5 \times 10^{12}$ cm^{-3}. Solid circle shows quantum mobility obtained from the resistivity at filling factor $\nu = 1/2$ measured in Ref. [1].

scattering rate is given by

$$\frac{1}{\tau_q} = \frac{2m^\star}{\pi \hbar^3} \int_0^{2k_F} \frac{dq}{\sqrt{4k_F^2 - q^2}} \langle |U(q)|^2 \rangle. \quad (10)$$

Background impurities. Since BIs far away from the quantum well contribute to μ_q significantly, excess electron screening cannot be ignored and the scattering potential is no longer given by Eq. (3). As a very good approximation, we can think of a perfect screening, such that the excess electron screening length is zero. However, the expression of scattering potential $U(q)$ in this approximation is still cumbersome so we leave it to the Supplemental Material [9] as a reference for an interested reader. As discussed above, two different impurity distributions, $N_2 = 0$ and $N_1 = N_2$, can describe the experimental μ reasonably well at $n_e < 1$. However, these distributions give very different values for μ_q, as shown in Fig. 3. Indeed, we find that $\mu_{q,BI}(N_2 = 0)$ (solid curve marked BI) is an order of magnitude smaller than $\mu_{q,BI}(N_1 = N_2)$ (dashed curve marked "BIBI More specifically, we find that $\mu_{q,BI}(N_2 = 0) \simeq 1.4 \, n_e^{0.85}$, whereas $\mu_{q,BI}(N_1 = N_2) \simeq 13.3 \, n_e^{0.87}$. As a result, future experiments measuring quantum mobility should be able to distinguish between these two distributions.

Remote donors. For quantum mobility limited by RI scattering, we use Eq. (23) from Ref. [3] valid at $1 - f = n_e/2n < 0.5$ for $n_e < 10$ [19],

$$\mu_{q,RI} = 6.5 \frac{e}{\hbar} \frac{n k_F d_w^3}{n_e} = 2.6 \times 10^3 \, n_e^{-7/2}, \quad (11)$$

where in the final expression we used $n = 15$, $k_F = \sqrt{2\pi n_e}$, and $d_w^{-1} = a n_e$ [8]. Even though Eq. (11) yields very large

$\mu_{q,RI} \simeq 56$ at $n_e = 3$, RI scattering is still expected to limit μ_q at higher n_e, see Fig. 3.

Interface roughness and alloy disorder. Contributions from IR and AD can be calculated using Eqs. (8)–(10). In particular, we find that $\mu_{q,IR} \simeq 1.2\mu_{IR}$ and $\mu_{q,AD} \simeq 1.3\mu_{AD}$. As shown in Fig. 3, these contributions are considerably smaller than the RI contribution at all relevant n_e. As a result, one expects a crossover from BI-limited to RI-limited quantum mobility for either model of BI distribution. The value and position of the maximum at the quantum mobility crossover should yield information on the BI distribution.

Next, we comment on the relation between the quantum mobility and the mobility of composite fermions μ_{CF} at filling factor $\nu = 1/2$. By comparing the expression of the longitudinal resistivity at $\nu = 1/2$, Eq. (5.11) of Ref. [27],

$$\rho_{1/2} = \frac{n_i}{n_e} \frac{1}{k_F z} \frac{2\sqrt{2}\pi\hbar}{e^2}, \quad (12)$$

and the expression for quantum mobility, Eq. (6) in Ref. [3],

$$\mu_q = \frac{2e}{\pi\hbar} \frac{k_F z}{n_i}, \quad (13)$$

one can conclude that

$$\mu_q = \frac{4\sqrt{2}}{en_e\rho_{1/2}}, \quad (14)$$

which implies that $\mu_q = 4\sqrt{2}\mu_{CF}$. Here, n_i is the 2D concentration of random impurities in a thin layer at a distance z away from the center of the quantum well. To obtain $\rho_{1/2}$ and μ_q^{-1} for impurities with 3D concentration $N(z)$, one should replace n_i by $N(z)dz$ and integrate over z [28]. This integration does not change the relation Eq. (14) between μ_q and $\rho_{1/2}$, so it holds for both BI and RI scattering [29].

From the experimental data in Ref. [1], the longitudinal resistance is $R_{1/2} = 35 \, \Omega$ at $\nu = 1/2$ and $n_e = 1$. Using the geometry of experiments in Ref. [1], we estimate $\rho_{1/2} \approx 2.5R_{1/2}$. As a result, the quantum mobility at $n_e = 1$ is estimated as $\mu_q = 4.0$. This data point, filled circle in Fig. 3, falls in between our predictions for $N_2 = 0$ and $N_1 = N_2$. To fit this point, while keeping μ the same as shown in Figs. 1 and 2, we need $N_1 \approx 4 \times 10^{13} \, cm^{-3}$ and $N_2 \approx 4 \times 10^{12} \, cm^{-3}$.

Finally, we mention that hydrodynamics [30] or scattering on oval defects [31] might affect the zero-field resistivity and, as a result, the inferred mobility. Both mechanisms manifest as negative magnetoresistance in weak magnetic field [31–37] which can also be seen in Fig. 3(b) of Ref. [1]. However, since no experimental studies of this magnetoresistance are yet available, we cannot comment on its origin.

In summary, we have examined roles of different scattering sources on the transport and quantum mobilities in the generation of ultrahigh mobility GaAs/Al$_{0.12}$As$_{0.88}$ quantum wells [1]. While at lower electron densities, both mobilities are limited by BI scattering, IR (remote impurity) scattering is the likely source limiting transport (quantum) mobility at large electron densities. Our predictions for quantum mobility are in agreement with the value estimated from the mobility of the composite fermions at filling factor $\nu = 1/2$ in a sample with $n_e = 1 \times 10^{11} \, cm^{-2}$ [1]. Future measurements of quantum mobility should provide insight on the distribution of BIs in the GaAs quantum well and in the AlGaAs barriers.

[1] Y. J. Chung, K. A. Villegas Rosales, K. W. Baldwin, P. T. Madathil, K. W. West, M. Shayegan, and L. N. Pfeiffer, Nat. Mater. **20**, 632 (2021).

[2] We note that both AD and IR scattering were not considered to be limiting factors in theories considering structures with mobilities even higher than reported in Ref. [1] (see, e.g., Ref. [38]).

[3] M. Sammon, M. A. Zudov, and B. I. Shklovskii, Phys. Rev. Materials **2**, 064604 (2018).

[4] Y. J. Chung, K. A. Villegas Rosales, K. W. Baldwin, K. W. West, M. Shayegan, and L. N. Pfeiffer, Phys. Rev. Materials **4**, 044003 (2020).

[5] T. Akiho and K. Muraki, Phys. Rev. Applied **15**, 024003 (2021).

[6] T. Akiho and K. Muraki, arXiv:2203.14575.

[7] Such a design, which is a special case of a short-period GaAs/AlAs superlattice [39,40], was realized in single heterointerfaces doped on one side in the 1990s [41,42].

[8] The condition $k_F w = 3.9$ defines maximum electron density at which the second subband of the GaAs quantum well remains unoccupied, where the dependence $d_w^{-1} = an_e$, where $a = 3.55$ nm, is governed by electrostatics. These conditions

were obtained from the fits to experimental data [1], see Supplemental Material [9].

[9] See Supplemental Material at http://link.aps.org/supplemental/10.1103/PhysRevMaterials.6.L061001 for constraints of samples parameters and the derivation of scattering potential.

[10] In our calculations, we ignore the density dependence of the effective mass, which is rather weak in the considered density range [43–47].

[11] M. Jonson, J. Phys. C: Solid State Phys. **9**, 3055 (1976).

[12] A. Gold, Solid State Commun. **60**, 531 (1986).

[13] A. Gold, Phys. Rev. B **35**, 723 (1987).

[14] A. Gold, Z. Phys. B **74**, 53 (1989).

[15] A. Gold, JETP Lett. **98**, 416 (2013).

[16] This uniform impurity concentration is also close to a recent estimate found in Ref. [17]. However, they used fixed quantum well width $w = 30$ nm in the calculations, while we take into account the density dependence such that $k_F w = 3.9$.

[17] S. Ahn and S. Das Sarma, Phys. Rev. Materials **6**, 014603 (2022).

[18] I. A. Dmitriev, A. D. Mirlin, D. G. Polyakov, and M. A. Zudov, Rev. Mod. Phys. **84**, 1709 (2012).

[19] Equations (22) and (23) in Ref. [3] apply to a single doping layer. Here, we consider two doping layers playing the same role, so the mobility is reduced by 2.

[20] H. Sakaki, T. Noda, K. Hirakawa, M. Tanaka, and T. Matsusue, Appl. Phys. Lett. **51**, 1934 (1987).

[21] D. Kamburov, K. W. Baldwin, K. W. West, M. Shayegan, and L. N. Pfeiffer, Appl. Phys. Lett. **109**, 232105 (2016).

[22] J. M. Li, J. J. Wu, X. X. Han, Y. W. Lu, X. L. Liu, Q. S. Zhu, and Z. G. Wang, Semicond. Sci. Technol. **20**, 1207 (2005).

[23] R. Gottinger, A. Gold, G. Abstreiter, G. Weimann, and W. Schlapp, Europhys. Lett. **6**, 183 (1988).

[24] D. R. Luhman, D. C. Tsui, L. N. Pfeiffer, and K. W. West, Appl. Phys. Lett. **91**, 072104 (2007).

[25] V. Umansky and M. Heiblum, MBE growth of high-mobility 2DEG, in *Molecular Beam Epitaxy: From research to mass production*, edited by M. Henini (Elsevier Inc., Amsterdam, 2013), pp. 121–137.

[26] T. Ando, J. Phys. Soc. Jpn. **51**, 3900 (1982).

[27] B. I. Halperin, P. A. Lee, and N. Read, Phys. Rev. B **47**, 7312 (1993).

[28] To avoid the divergence at $z = 0$, one can average z in the denominator using $\langle z \rangle = \int dz' |\psi(z')|^2 |z - z'|$, where $\psi(z)$ is the wave function along z direction.

[29] On the other hand, AD and IR do not change the 2D electron concentration inside the quantum well, so do not contribute to the gauge field fluctuations and $\rho_{1/2}$.

[30] P. S. Alekseev, Phys. Rev. Lett. **117**, 166601 (2016).

[31] L. Bockhorn, I. V. Gornyi, D. Schuh, C. Reichl, W. Wegscheider, and R. J. Haug, Phys. Rev. B **90**, 165434 (2014).

[32] Y. Dai, R. R. Du, L. N. Pfeiffer, and K. W. West, Phys. Rev. Lett. **105**, 246802 (2010).

[33] A. T. Hatke, M. A. Zudov, L. N. Pfeiffer, and K. W. West, Phys. Rev. B **83**, 121301(R) (2011).

[34] L. Bockhorn, P. Barthold, D. Schuh, W. Wegscheider, and R. J. Haug, Phys. Rev. B **83**, 113301 (2011).

[35] A. T. Hatke, M. A. Zudov, J. L. Reno, L. N. Pfeiffer, and K. W. West, Phys. Rev. B **85**, 081304(R) (2012).

[36] Q. Shi, P. D. Martin, Q. A. Ebner, M. A. Zudov, L. N. Pfeiffer, and K. W. West, Phys. Rev. B **89**, 201301(R) (2014).

[37] Q. Shi, M. A. Zudov, L. N. Pfeiffer, and K. W. West, Phys. Rev. B **90**, 201301(R) (2014).

[38] E. H. Hwang and S. Das Sarma, Phys. Rev. B **77**, 235437 (2008).

[39] T. Baba, T. Mizutani, and M. Ogawa, Jpn. J. Appl. Phys. **22**, L627 (1983).

[40] K.-J. Friedland, R. Hey, H. Kostial, R. Klann, and K. Ploog, Phys. Rev. Lett. **77**, 4616 (1996).

[41] R. R. Du, H. L. Stormer, D. C. Tsui, L. N. Pfeiffer, and K. W. West, Phys. Rev. Lett. **70**, 2944 (1993).

[42] L. N Pfeiffer (private communication).

[43] P. Coleridge, M. Hayne, P. Zawadzki, and A. Sachrajda, Surf. Sci. **361-362**, 560 (1996).

[44] Y.-W. Tan, J. Zhu, H. L. Stormer, L. N. Pfeiffer, K. W. Baldwin, and K. W. West, Phys. Rev. Lett. **94**, 016405 (2005).

[45] A. T. Hatke, M. A. Zudov, J. D. Watson, M. J. Manfra, L. N. Pfeiffer, and K. W. West, Phys. Rev. B **87**, 161307(R) (2013).

[46] A. V. Shchepetilnikov, D. D. Frolov, Y. A. Nefyodov, I. V. Kukushkin, and S. Schmult, Phys. Rev. B **95**, 161305(R) (2017).

[47] X. Fu, Q. A. Ebner, Q. Shi, M. A. Zudov, Q. Qian, J. D. Watson, and M. J. Manfra, Phys. Rev. B **95**, 235415 (2017).